Journal of Power Sources 192 (2009) 391–395

Contents lists available at ScienceDirect

Journal of Power Sources

journal homepage: www.elsevier.com/locate/jpowsour

Short communication

Investigation of PtCoCr/C catalysts for methanol electro-oxidation identified by a thin film combinatorial method

Min Ku Jeon, James S. Cooper, Paul J. McGinn*

Department of Chemical and Biomolecular Engineering, University of Notre Dame, Notre Dame, IN 46556, USA

ARTICLE INFO

Article history:
Received 19 January 2009
Received in revised form 23 February 2009
Accepted 24 February 2009
Available online 14 March 2009

Keywords:
Methanol electro-oxidation
Direct methanol fuel cell
Combinatorial synthesis
High-throughput screening
Electrocatalyst

ABSTRACT

The ternary Pt–Co–Cr system was investigated for suitability as a methanol electro-oxidation reaction (MOR) catalyst by combinatorial synthesis and high-throughput screening method. A PtCoCr thin film library was prepared by a multi-target sputtering technique while parallel characterization was performed using a multichannel multielectrode analyzer. The highest MOR activity was observed in the $Pt_{30}Co_{30}Cr_{40}$ composition after a conditioning process. The high MOR activity of the thin film $Pt_{30}Co_{30}Cr_{40}$ composition was verified in a powder version of the alloy. In 20 h chronoamperometry tests, the MOR activity of the $Pt_{30}Co_{30}Cr_{40}$ powder catalyst alloy was 10.3 A $g^{-1}_{\text{noble metal}}$, which was 160% higher than the 4.03 A $g^{-1}_{\text{noble metal}}$ value of the PtRu/C catalyst, suggesting that PtCoCr alloys are promising candidates as Ru-free MOR catalysts. The effect of the conditioning process was also investigated, revealing that dissolution and oxidation of surface Co and Cr occurs during conditioning. After conditioning, the activity of 900 °C reduced $Pt_{30}Co_{30}Cr_{40}$ catalyst dramatically increased by 26.8 times from 0.0765 to 2.13 A $g^{-1}_{\text{cat.}}$ at 600 s of the chronoamperometry tests.

1. Introduction

Development of catalysts to promote the methanol electro-oxidation reaction (MOR) is the focus of much research for direct methanol fuel cells (DMFCs) application. Pure Pt is not suitable as an anode catalyst in DMFCs due to rapid poisoning by intermediate CO [1]. Introduction of Pt–Ru alloy catalysts significantly improves the CO tolerance of Pt-based catalysts [2–5]. Even higher MOR activity of PtRu catalysts was achieved by adding transition metals [6–9] to form ternary alloys such as PtRuFe [10,11], PtRuCo [12–14], PtRuW [12,15], PtRuMo [9,16], and PtRuNi [17–19]. However, research suggests that Ru in the anode is dissolved during DMFC operation [20,21] and that the dissolved Ru is transported across the membrane and reduced on the cathode electrode [22,23]. This phenomenon is considered to be one of the major issues in performance degradation of DMFCs, so a Ru-free catalyst is desirable to eliminate this degradation mechanism. Research on Ru-free MOR catalysts is not extensive but a few encouraging results have been reported. For example, enhancement in the MOR activity by alloying Pt with transition metals such as Co, Ni, Fe, and Cu was reported [24]. Significantly improved MOR activity was reported in Pt–Pb system [25–27], which exhibited 2–97 times higher activity than PtRu catalyst although it has a higher onset potential [25].

Development of new catalysts in such systems is both time-consuming and expensive due to the vast number of possible combinations of metals. The time and cost can be efficiently lessened by a combinatorial synthesis and high-throughput screening approach. Hence in the Pt–Pb system such approaches are already beginning to emerge [28,29]. The combinatorial method was first applied to electrocatalysts by Reddington et al. [30], and since that report various synthesis (e.g., solution dispensing [31], physical vapor deposition [12,32], and electrodeposition [33]) and characterization methods (e.g., optical screening [30,34], scanning electrochemical microscopy [35], multielectrode half cell [36,37], and multielectrode full cell [38]) have been developed [39]. Among these various methods, in the present study, we employed physical vapor deposition (sputtering) and a multielectrode half cell system due to their benefit for reproducible preparation of discrete catalyst compositions and quantitative, parallel, and quick analysis of the combinatorial library, respectively. Recently, by using a thin film combinatorial method, a promising Ru-free MOR catalyst was identified in the ternary Pt–Ni–Cr system [40]. The results obtained from the thin film combinatorial library were verified by synthesizing a powder version, which exhibited performance comparable with a PtRu powder based on a catalyst mass scale (A $g^{-1}_{\text{cat.}}$) and even better performance on a noble metal mass basis (A $g^{-1}_{\text{noble metal}}$) [41].

In the present study, we explored the ternary Pt–Co–Cr system for potential MOR catalysts via synthesis and parallel characterization of a combinatorial thin film library. This system was previously reported as a promising oxygen electro-reduction reaction catalyst

* Corresponding author. Tel.: +1 574 631 6151; fax: +1 574 631 8366.
E-mail address: mcginn.1@nd.edu (P.J. McGinn).

0378-7753/$ – see front matter © 2009 Elsevier B.V. All rights reserved.
doi:10.1016/j.jpowsour.2009.02.087

[42]. The same library was investigated for its MOR activity and the best composition in the library was characterized in a powder form. Because a conditioning process was reported to improve the MOR activity of thin film catalysts [43], powder conditioning was investigated to provide better performance correlation between thin film and powder catalysts.

2. Experimental

2.1. Thin film library synthesis and characterization

The library preparation procedure [42] has been described previously. Building a thin film combinatorial library starts by using photoresist to develop a pattern of titanium nitride leads and pads on a 50 mm silicon wafer. These capture pads are hexagonal (0.026 cm^2) with a nearest neighbor distance of 1.6 mm. Around the periphery of the wafer there is a ring of electrical contact pads that are the connection points (through a series of pogo probes) to the multichannel potentiostat. The network of electrical traces connects each hexagonal capture pad with its respective circular contact pad. Outside of the combinatorial pattern are 12 composition pads that are captured with a 7th mask. A fixed reference composition, typically Pt, is deposited at these 12 locations to permit easy comparison between libraries. After deposition of the capture pads, Pt, Co, and Cr targets were sputtered through a series of shadow masks to fabricate 63 discrete pads of different composition as well as the reference pads. A computer program sequentially selects gun and mask combinations to deposit a series of multilayer samples with varying compositions on the substrate. The deposited library was annealed ex situ after deposition in a 10^{-6} Torr vacuum. The annealing schedule was 550 °C for 4 h followed by a rapid high temperature anneal at 900 °C for 5 min to achieve homogeneous crystalline films since the as-deposited library consists of multilayers of Pt, Co, and Cr.

Parallel potentiostatic analysis to measure MOR activity of the deposited compositions was performed with a commercial multielectrode system (Scribner Associates model 900B Multichannel Microelectrode Analyzer (MMA)) which can control 100 channels at a time. MOR activity was measured at room temperature by potential cycling between −0.06 and 1.34 V (vs. reference hydrogen electrode (RHE)) in nitrogen purged 0.5 M H_2SO_4 + 0.5 M methanol electrolyte solution. Dry nitrogen was bubbled through the electrolyte until a stable open circuit potential was attained, which usually required at least 10 min. The cell potential at all of the catalyst pads was then set and held at 0.04 V (vs. RHE) for an additional 10 min before testing. Testing began by acquiring cyclic voltammograms at room temperature between −0.06 and +1.34 V (vs. RHE), at a scan rate of 10 mV s^{-1}, until a stable curve was reproducibly measured from all of the catalyst pads. This usually required 10–20 cycles. For screening of MOR activity, the potential was again held at 0.04 V (vs. RHE) while methanol was introduced into the electrolyte to achieve an equivalent to 0.5 M solution. After allowing the solution to homogenize and the measured currents to stabilize, the potential was again swept from −0.06 to 1.34 V (vs. RHE) at 10 mV s^{-1} until stable curves were again measured from all of the catalyst pads.

After the initial characterization, the library was subjected to a "conditioning" process, which consisted of potential cycling at 60 °C between −0.06 and 1.34 V (vs. RHE) for 10 cycles at a scan rate of 10 mV s^{-1}. After the conditioning, MOR activity was measured again at room temperature under the same conditions described above. The current density values from the thin film libraries are based on the geometric area of the sample pad (0.026 cm^2) and not the active area. The active area of platinum surfaces is usually determined by examining a monolayer adsorption during a potential sweep [44–46]. Assuming that a monolayer of protons is adsorbed onto active Pt sites, the area under the curve for this region is directly proportional to the active area. The present combinatorial approach necessitates reporting currents from widely varying compositions, including some with no platinum at all. Unfortunately, for catalysts with little to no Pt there is an overpotential for the adsorption of hydrogen so this method is inaccurate at determining their active area. Other methods to determine roughness, such as DEMS [47] or STM [48] are not compatible with the present combinatorial testing approach. Instead, compositions were ranked based on their onset potentials and peak methanol oxidation current densities for a few reasons. The onset potential was examined because it is not influenced by any change in the surface roughness. Previous testing on thin film libraries showed there was a strong correlation between the peak current density and the current density observed after a 5 min chronoamperometric experiment at 0.74 V [11]. Finally, it is important note that the thin film libraries are used for the purpose of screening compositions, i.e., to distinguish the most active compositions. That is why it is advisable to follow thin film studies with an investigation of the most promising compositions in powder form in order to validate the thin film results and perform more extensive electrochemical characterization.

2.2. Powder synthesis and characterization

After being identified in the thin film combinatorial library as the most active catalyst composition for the MOR, $Pt_{30}Co_{30}Cr_{40}$ powder was synthesized by a conventional $NaBH_4$ reduction method ("PtCoCr–$NaBH_4$") [49]. $H_2PtCl_6{\cdot}6H_2O$, $Co(NO_3)_2{\cdot}6H_2O$, and $Cr(NO_3)_3{\cdot}9H_2O$ were used as precursors of Pt, Co, and Cr, respectively. The precursors were dissolved in a mixture of deionized (DI) water and methanol (80:1, v/v), and then carbon support (Vulcan XC-72R) was added to the solution. The precursor concentration was 0.573, 0.573, and 0.763 mmol L^{-1} for the Pt, Co, and Cr precursors, respectively. The mixture was sonicated and stirred for 30 min to achieve homogeneous mixing. 0.2 M $NaBH_4$ solution was added to the mixture as a reducing agent. The mixture was further stirred for 1 h to complete the reaction. All of the reactions were performed at room temperature. The final mixture was filtered and washed by DI water, and then dried at 100 °C in an oven overnight. Loading of total metals was adjusted as 20 wt.% of the total catalyst mass.

Electrochemical tests were performed in a beaker-type three electrode cell. A glassy carbon electrode (3 mm diameter, BAS Co., Ltd., MF-2012) was used as the working electrode. Catalyst layers were formed by a thin-film method [50]. The catalysts were dispersed in a mixture of DI water and Nafion ionomer solution. The dispersion mass ratio was 1 (Nafion):11.4 (catalyst):1140 (water). The dispersion was sonicated for homogeneous mixing and then a small amount of the dispersion was dripped on the working electrode. After air drying, a 5 wt.% Nafion ionomer solution was dripped on the catalyst layer to stabilize it. The glassy carbon working electrode catalyst loading was 1.39 $mg_{cat.}$ cm^{-2} electrode. Platinum mesh and saturated calomel electrodes were used as the counter and reference electrodes, respectively.

The PtCoCr–$NaBH_4$ catalyst powder was subject to a conditioning process. First, the PtCoCr–$NaBH_4$ was annealed at 900 °C for 5 min under H_2/Ar (5.2 mol% H_2) flow to achieve a high degree of alloying. Prior to annealing at 900 °C, the furnace was purged with the H_2/Ar gas for 1 h. To minimize the catalyst time at 900 °C, quick insertion into and removal from the furnace hot zone was achieved via an external magnetic pushing device. The resulting annealed catalyst is named as "PtCoCr-900". The PtCoCr-900 catalyst was conditioned by potential cycling between −0.06 and 1.34 V (vs. RHE) for 10 cycles at a scan rate of 10 mV s^{-1} in 60 °C 0.5 M H_2SO_4. The conditioned PtCoCr-900 catalyst is termed "PtCoCr-cond."

Cyclic voltammetry (CV) and MOR activity were measured before and after the conditioning process. For the CV, potential was cycled at 50 mV s^{-1} between 0 and 0.8 V (vs. RHE) for 50 cycles at room temperature in 0.5 M H_2SO_4 electrolyte. Chronoamperometry tests were performed by keeping the potential of the working electrode at 0.6 V (vs. RHE) for 600 s in 1 M H_2SO_4 + 1 M methanol solution. All potentials in this paper were converted to RHE scale.

3. Results and discussion

The MOR activity test results of the combinatorial library are shown in Fig. 1. Before the conditioning process (Fig. 1(a)), $Pt_{20}Co_{60}Cr_{20}$ composition showed the highest MOR activity. But this composition showed poor performance after the conditioning process (Fig. 1(b)) due to corrosion. The corrosion performance of this library was shown in an earlier report (Fig. 6b of Ref. 42), and the poor corrosion score of the $Pt_{20}Co_{60}Cr_{20}$ composition suggests that significant dissolution of Co and Cr during the conditioning process caused the loss of MOR activity. The highest MOR activity after conditioning was observed for the $Pt_{30}Co_{30}Cr_{40}$ composition, which also exhibited an excellent corrosion score [42]. This composition exhibited a significant increase of current density from 3.8×10^{-4} to 2.9×10^{-3} A cm^{-2} after the conditioning process. Further investigation on the performance of the $Pt_{30}Co_{30}Cr_{40}$ composition was performed on the alloy in powder form.

X-ray diffraction results of the PtCoCr–$NaBH_4$, and PtCoCr-900 powder catalysts are shown in Fig. 2. The (1 1 1) peak was observed at 39.85° in the PtCoCr–$NaBH_4$ catalyst, which is a slightly higher 2θ value than 39.48° in the Pt/C catalyst [41]. This slight shift indicates only slight alloying of Co and Cr with Pt was achieved [41]. The (1 1 1) peak shifted to 41.41° in the PtCoCr-900 catalyst due to extensive alloying from the 900 °C anneal. In the PtCoCr-900 catalyst, new peaks were observed corresponding to formation of ordered cubic Pt_3M (M is Co and/or Cr) and/or tetragonal PtM phases. The peaks of the Pt_3M and PtM phases (denoted by '*' in Fig. 2) were not distinguishable due to very close peak positions and low intensities. Some other peaks that do not match to the intermetallic phases (Pt_3M and PtM) could be assigned as Cr_2O_3 peaks (JCPDS-ICDD #01-073-6214, denoted by '+' in Fig. 2). The formation of Cr_2O_3 means that the annealing conditions were not sufficient to reduce the Cr_2O_3 into metallic Cr. The source of oxygen might be the precursor, which means Cr was not fully reduced by the $NaBH_4$ reduction process, and/or from trace oxygen remaining inside the furnace. The above results show that the structure of the PtCoCr-900 catalyst mainly consists of the disordered PtCoCr solid solution along with a minor fraction of the ordered Pt_3M and PtM alloy phases and Cr_2O_3. Crystallite sizes of the catalysts were calculated from (1 1 1) peaks near 40° by using the Scherrer equation [51], yielding 2.6 [41], 2.2, and 7.3 nm for the Pt/C, PtCoCr–$NaBH_4$, and PtCoCr-900 catalysts, respectively.

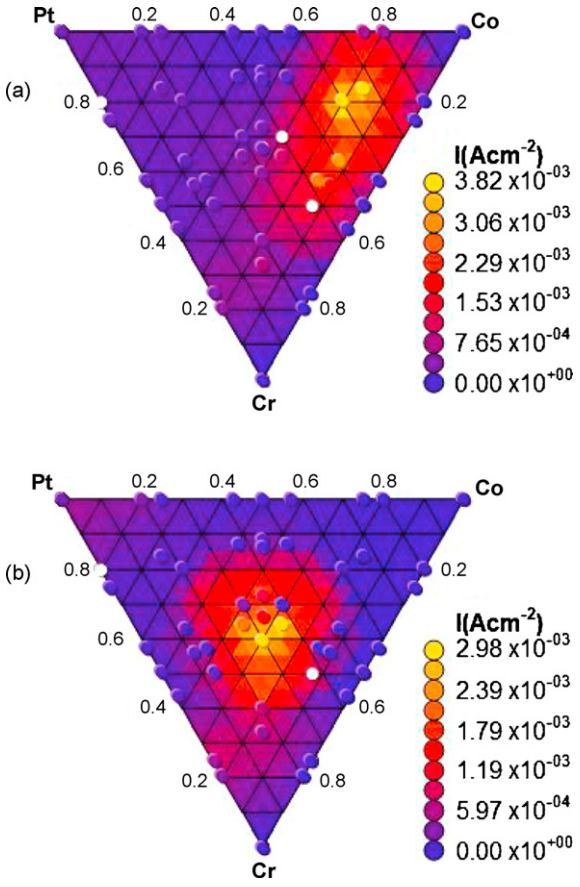

Fig. 1. The MOR activity measurement results of the Pt–Co–Cr thin film combinatorial library (a) before and (b) after the conditioning process.

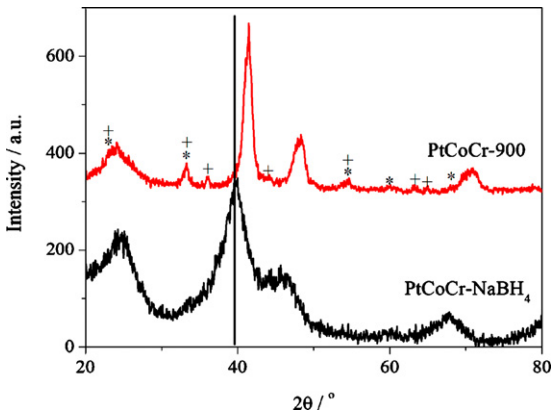

Fig. 2. The XRD results of the PtCoCr–$NaBH_4$ and PtCoCr-900 catalysts. The tetragonal PtCo peaks are denoted by asterisks and the superlattice of the PtCo phase by a plus sign. Vertical line shows peak position of pure Pt.

Fig. 3(a) shows the MOR activity test results measured by keeping the potential of the working electrodes at 0.6 V for 600 s. The data for Pt/C and PtRu/C catalysts reported in an earlier study [41] are also included for comparison. In contrast to the current densities of PtRu/C and Pt/C which decrease continuously, the PtCoCr–$NaBH_4$ catalyst shows almost a flat response over the 600 s period, suggesting low susceptibility to poisoning by intermediate CO. The activity of the PtCoCr–$NaBH_4$ at 600 s was 3.14 A $g^{-1}_{cat.}$, which is 84% of the 3.75 A $g^{-1}_{cat.}$ value for the PtRu/C catalyst. On a g-noble metal scale, the PtCoCr–$NaBH_4$ catalyst exhibited 38% higher activity (26.0 A $g^{-1}_{noble\ metal}$) than the PtRu/C catalyst (18.8 A $g^{-1}_{noble\ metal}$). In the PtCoCr-900 catalyst, the MOR activity was very low due to a decrease of surface area resulting from the particle size increase and formation of a Co and Cr oxides surface (see discussion of Fig. 4). But the low MOR activity of the PtCoCr-900 catalyst, 0.0765 A $g^{-1}_{cat.}$, dramatically increased to 2.13 A $g^{-1}_{cat.}$ (27.8 times) after the conditioning process. Further discussion on the effect of conditioning is included below. Prolonged chronoamperometry testing was performed to elucidate the apparent decay-free performance of the PtCoCr catalysts. Fig. 3(b) shows 20 h chronoamperometry results at 0.6 V for the PtRu/C and PtCoCr–$NaBH_4$ catalysts, which are shown on a g-noble metal scale (A $g^{-1}_{noble\ metal}$). The PtCoCr–$NaBH_4$ catalyst began to decay after 30 min operation, and the rate of performance decay was similar to that of the PtRu/C catalyst. The current density of the PtCoCr–$NaBH_4$ catalyst after 20 h was 10.3 A $g^{-1}_{noble\ metal}$, which was

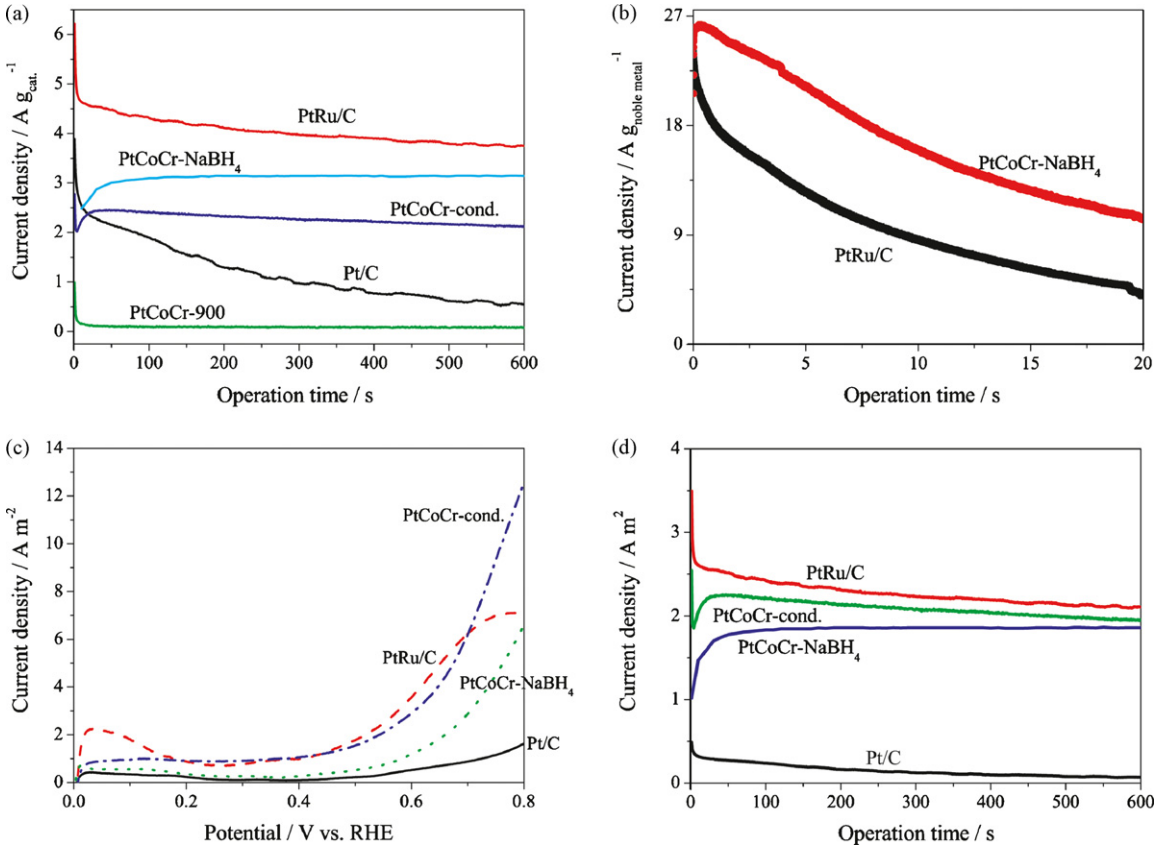

Fig. 3. (a) The chronoamperometry results of the PtCoCr–$NaBH_4$, PtCoCr-900, PtCoCr-cond., Pt/C, and PtRu/C catalysts measured for 600 s. The results of the PtRu/C and Pt/C catalysts are from Ref. [26]. (b) The 20 h chronoamperometry results of the PtRu/C and PtCoCr–$NaBH_4$ catalysts. Both tests were performed by keeping the working electrode at 0.6 V in the 1 M H_2SO_4 + 1 M methanol electrolyte. (c) CV results of the Pt/C, PtRu/C, PtCoCr–$NaBH_4$, and PtCoCr-cond. catalysts measured by potential cycling between 0 and 0.8 V (vs. RHE) at a scan rate of 50 mV s^{-1} in 1 M H_2SO_4 + 1 M methanol electrolyte. The results are shown on specific activity scale. (d) Data from (a) replotted in terms of specific activity.

160% higher than the 4.03 A $g_{noble\ metal}^{-1}$ value of the PtRu/C catalyst. These results show that the PtCoCr catalyst exhibits low CO poisoning and is a promising Ru-free MOR catalyst. The MOR performance was also compared in terms of specific activity by dividing the mass activities by electrochemically active surface area (EAS). Calculation of EAS values was based on the CV results which are shown in Fig. 4, yielding values of 7.96, 1.78, 1.69, and 1.09 m^2 $g_{cat.}^{-1}$ for the Pt/C, PtRu/C, PtNiCr–$NaBH_4$, and PtNiCr-cond. catalysts, respectively. For the values of Pt/C and PtRu/C, we referred to our previous study [41]. It should be noted that the calculation of the EAS values was based on 210 μC charge for desorption of monolayer H^+ on polycrystalline Pt although this value is not precise in alloy catalysts. The EAS value of the PtCoCr-900 catalyst was not calculated due to an indistinguishable H^+ desorption area. Fig. 3(c) shows the CV results performed in 1 M H_2SO_4 + 1 M methanol solution on a specific activity scale. For the PtRu/C catalyst, we referred our previous report [52]. At 0.6 V, the order of specific activities was PtRu/C (3.57) > PtCoCr-cond. (2.91) > PtCoCr–$NaBH_4$ (1.17) > Pt/C (0.520). The chronoamperometry results of Fig. 3(a) are replotted in Fig. 3(d) as a function of their specific activity. The order of activity was not changed. At 600 s operation, the specific activities were 0.0685, 2.11, 1.86, and 1.95 A m^{-2} for the Pt/C, PtRu/C, PtCoCr–$NaBH_4$, and PtCoCr-cond. catalysts, respectively. Although the PtCoCr-cond. catalyst exhibited much higher specific activity than the PtCoCr–$NaBH_4$ catalyst in the cyclic test, their performance did not show much difference in the chronoamperometric tests. This result shows that the presumably higher degree of alloying is not beneficial for improving CO tolerance.

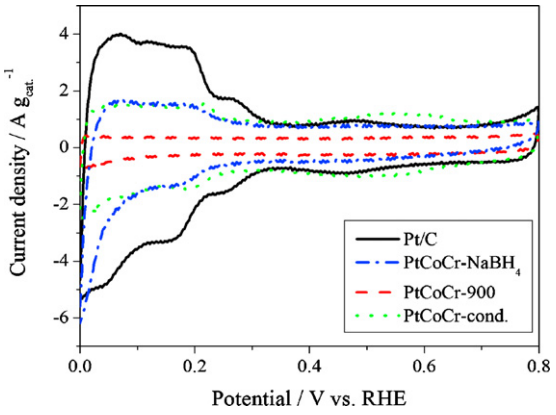

Fig. 4. The CV results of the Pt/C, PtCoCr–$NaBH_4$, PtCoCr-900, and PtCoCr-cond. catalysts. The tests were performed by potential cycling between 0 and 0.8 V (vs. RHE) at a scan rate of 50 mV s^{-1}. 0.5 M H_2SO_4 solution was used as the electrolyte.

The effect of conditioning was investigated by CV testing, with the results for Pt/C, PtCoCr–$NaBH_4$, PtCoCr-900 and PtCoCr-cond. catalysts being shown in Fig. 4. The PtCoCr-900 catalyst exhibited no specific peaks in the H^+ desorption range (0–0.3 V), which means a Co and Cr oxides rich surface was formed during the annealing process. But after conditioning, H^+ desorption peaks are clearly shown indicating that surface Co and Cr were dissolved during the conditioning process. In addition, in the PtCoCr-cond. catalyst, oxidation/reduction peaks were observed near 0.55 V, which is different from the pure Pt/C catalyst. Duong et al. [53] showed that Co

oxides are dissolved during potential cycling between 0 and 1.4 V for 40 cycles. In their Pt_3Co catalyst [53], a small oxidation peak is observed near 0.55 V which disappears with increasing number of potential cycles between 0 and 1.4 V to form a Pt skin surface. Therefore, it can be recognized that the oxidation/reduction peaks of the PtCoCr-cond. catalyst came from the oxides of Co and Cr. In addition, it can be concluded that the performance improvement via the conditioning process was induced by dissolution and oxidation of Co and Cr.

In earlier studies it was shown that the performance of Pt–M and Pt–M_1–M_2 alloys synthesized by the borohydride reduction technique depends on the amount of excess $NaBH_4$ used during the reduction process [41,49]. This aspect of the process was not optimized for PtCoCr in the present study.

The performance improvement resulting from the anodic conditioning treatment is similar to what was recently reported for PtNiCr alloys [43]. In that study it was found that it is possible to optimize the voltage used in the anodic "conditioning" treatment to maximize the current density. The anodic conditioning process appears to lead to the formation of reversible (hydrous) oxides. In that study it was shown that the performance of Pt–Ru alloys also benefits from such a treatment. The optimum voltage likely depends on the alloy composition. Both the $NaBH_4$ reduction and conditioning processes can be optimized to further enhance the performance of the $Pt_{30}Co_{30}Cr_{40}$ alloy.

4. Conclusions

The PtCoCr system was investigated to identify possible Ru-free MOR catalysts by a thin film combinatorial synthesis and high-throughput screening method. The $Pt_{30}Co_{30}Cr_{40}$ composition was identified as having the highest MOR activity among 63 different compositions in the combinatorial library. A powder version of $Pt_{30}Co_{30}Cr_{40}$ showed 160% higher activity ($10.3\ A\ g^{-1}_{\text{noble metal}}$) than a comparably synthesized PtRu/C catalyst ($4.03\ A\ g^{-1}_{\text{noble metal}}$) after 20 h of chronoamperometry tests. The positive effect of anodic conditioning observed in thin films was also verified in the powder version, resulting in a dramatic increase of the MOR mass activity (27.8 times). The improvement resulted from the dissolution and oxidation of surface Co and Cr oxides. These results show that the Pt–Co–Cr system is a promising candidate as a Ru-free MOR catalyst, and a suitable anodic conditioning process can improve the MOR activity of the Pt–Co–Cr catalysts.

Acknowledgements

This work was partially supported by the U.S. Army CECOM RDEC through Agreement DAAB07-03-3-K414 and by the Department of Defense and the Army Research Office through contract numbers W911QX06C0117 and W911NF08C0037. Such support does not constitute endorsement by the U.S. Army of the views expressed in this publication.

References

[1] A.S. Arico, S. Srinivasan, V. Antonucci, Fuel Cells 1 (2001) 133–161.
[2] M. Watanabe, S. Motoo, J. Electroanal. Chem. 60 (1975) 267–273.
[3] N.M. Markovic, H.A. Gasteiger, P.N. Ross Jr., Electrochim. Acta 40 (1995) 91–98.
[4] W. Chrzanowski, A. Wieckowski, Langmuir 14 (1998) 1967–1970.
[5] O.A. Petrii, J. Solid State Electrochem. 12 (2008) 609–642.
[6] E. Antolini, Appl. Catal. B: Environ. 74 (2007) 324–336.
[7] E. Antolini, Appl. Catal. B: Environ. 74 (2007) 337–350.
[8] U.B. Demirci, J. Power Sources 173 (2007) 11–18.
[9] C. Lamy, A. Lima, V. LeRhun, F. Delime, C. Coutanceau, J.-M. Léger, J. Power Sources 105 (2002) 283–296.
[10] M.K. Jeon, J.Y. Won, K.R. Lee, S.I. Woo, Electrochem. Commun. 9 (2007) 2163–2166.
[11] M.K. Jeon, K.R. Lee, H. Daimon, A. Nakahara, S.I. Woo, Catal. Today 132 (2008) 123–126.
[12] J.S. Cooper, P.J. McGinn, J. Power Sources 163 (2006) 330–338.
[13] P. Strasser, J. Comb. Chem. 10 (2008) 216–224.
[14] S. Pasupathi, V. Tricoli, J. Solid State Electrochem. 12 (2008) 1093–1100.
[15] C. Roth, M. Goetz, H. Fuess, J. Appl. Electrochem. 31 (2001) 793–798.
[16] A. Oliveira Neto, E.G. Franco, E. Arico, M. Linardi, E.R. Gonzalez, J. Eur. Ceram. Soc. 23 (2003) 2987–2992.
[17] J. Liu, J. Cao, Q. Huang, X. Li, Z. Zou, H. Yang, J. Power Sources 175 (2008) 159–165.
[18] J.H. Choi, K.W. Park, B.K. Kwon, Y.E. Sung, J. Electrochem. Soc. 150 (2003) A973–A978.
[19] Z. Wang, G. Yin, J. Zhang, Y. Sun, P. Shi, Electrochim. Acta 51 (2006) 5691–5697.
[20] M.K. Jeon, K.R. Lee, K.S. Oh, D.S. Hong, J.Y. Won, S. Li, S.I. Woo, J. Power Sources 158 (2006) 1344–1347.
[21] M.K. Jeon, J.Y. Won, K.S. Oh, K.R. Lee, S.I. Woo, Electrochim. Acta 53 (2007) 447–452.
[22] P. Piela, C. Eickes, E. Brosha, F. Garzon, P. Zelenay, J. Electrochem. Soc. 151 (2004) A2053–A2059.
[23] Y. Chung, C. Pak, G.S. Park, W.S. Jeon, J.R. Kim, Y. Lee, H. Chang, D. Seung, J. Phys. Chem. C 112 (2008) 313–318.
[24] E. Antolini, J.R.C. Salgado, E.R. Gonzalez, Appl. Catal. B: Environ. 63 (2006) 137–149.
[25] C. Roychowdhury, F. Matsumoto, V.B. Zeldovich, S.C. Warren, P.F. Mutolo, M. Ballesteros, U. Wiesner, H.D. Abruna, F.J. DiSalvo, Chem. Mater. 18 (2006) 3365–3372.
[26] S. Papadimitriou, A. Tegou, E. Pavildou, G. Kokkinidis, S. Sotiropoulos, Electrochim. Acta 52 (2007) 6254–6260.
[27] Z. Liu, B. Guo, S.W. Tay, L. Hong, X. Zhang, J. Power Sources 184 (2008) 16–22.
[28] J. Jin, M. Prochaska, D. Rochefort, D.K. Kim, L. Zhuang, F.J. DiSalvo, R.B. van Dover, H.D. Abruña, Appl. Surf. Sci. 254 (2007) 653–661.
[29] M. Chen, Z.-B. Wang, Y. Ding, G.-P. Yin, Electrochem. Commun. 10 (2008) 443–446.
[30] E. Reddington, A. Sapienza, B. Gurau, R. Viswanathan, S. Sarangapani, E.S. Smotkin, T.E. Mallouk, Science 280 (1998) 1735–1737.
[31] W.C. Choi, J.D. Kim, S.I. Woo, Catal. Today 74 (2002) 235–240.
[32] S. Guerin, B.E. Hayden, D. Pletcher, M.E. Rendall, J.-P. Suchsland, L.J. Williams, J. Comb. Chem. 8 (2006) 791–798.
[33] S. Jayaraman, S.-H. Baeck, T.F. Jaramillo, A. Kleinman-Shwarsctein, E.W. McFarland, Rev. Sci. Instrum. 76 (2005) 062227.
[34] J.M. Gregoire, M. Kostylev, M.E. Tague, P.F. Mutolo, R.B. van Dover, F.J. DiSalvo, H.D. Abruña, J. Electrochem. Soc. 156 (2009) B160–B166.
[35] M. Black, J. Cooper, P. McGinn, Meas. Sci. Technol. 16 (2005) 174–182.
[36] S. Guerin, B.E. Hayden, C.E. Lee, C. Mormiche, J.R. Owen, A.E. Russell, J. Comb. Chem. 6 (2004) 149–158.
[37] M.D. Fleischauer, T.D. Hatchard, G.P. Rockwell, J.M. Topple, S. Trussler, S.K. Jericho, M.H. Jericho, J.R. Dahn, J. Electrochem. Soc. 150 (2003) A1465–A1469.
[38] R. Liu, E.S. Smotkin, J. Electroanal. Chem. 535 (2002) 49–55.
[39] E.S. Smotkin, R.R. Diaz-Moralez, Annu. Rev. Mater. Res. 33 (2003) 557–579.
[40] J.S. Cooper, M.K. Jeon, P.J. McGinn, Electrochem. Commun. 10 (2008) 1545–1547.
[41] M.K. Jeon, Y. Zhang, P.J. McGinn, Electrochim. Acta 54 (2009) 2837–2842.
[42] J.S. Cooper, P.J. McGinn, Appl. Surf. Sci. 254 (2007) 662–668.
[43] M.K. Jeon, P.J. McGinn, J. Power Sources 188 (2009) 427–432.
[44] T. Biegler, D.A.J. Rand, R. Woods, J. Electroanal. Chem. 29 (1971) 269–277.
[45] B.E. Conway, H. Angerstein-Kozlowska, Acc. Chem. Res. 14 (1981) 49–56.
[46] R.P. Šimpraga, B.E. Conway, Electrochim. Acta 43 (1998) 3045–3058.
[47] Z. Jusys, T.J. Schmidt, L. Dubau, K. Lasch, L. Jörissen, J. Garche, R.J. Behm, J. Power Sources 105 (2002) 297–304.
[48] H.M. Saffarian, R. Srinivasan, D. Chu, S. Gilman, Electrochim. Acta 44 (1998) 1447–1454.
[49] M.-S. Hyun, S.-K. Kim, B. Lee, D. Peck, Y. Shul, D. Jung, Catal. Today 132 (2008) 138–145.
[50] T.J. Schmidt, H.A. Gasteiger, G.D. Stäb, P.M. Urban, D.M. Kolb, R.J. Behm, J. Electrochem. Soc. 145 (1998) 2354–2358.
[51] C.Z. He, H.R. Kunz, J.M. Fenton, J. Electrochem. Soc. 144 (1997) 970–979.
[52] M.K. Jeon, J.S. Cooper, P.J. McGinn, J. Power Sources 185 (2008) 913–916.
[53] H.T. Duong, M.A. Rigsby, W.-P. Zhou, A. Wieckowski, J. Phys. Chem. C 111 (2007) 13460–13465.